Control of Calcite Crystal Morphology by a Peptide Designed To Bind to a Specific Surface

Daniel B. DeOliveira and Richard A. Laursen*

Contribution from the Department of Chemistry, Boston University, Boston, Massachusetts 02215

Received July 8, 1997[⊗]

Abstract: Many organisms contain proteins which regulate the size and shape of inorganic crystals in their skeletal elements, most likely through specific protein−crystal surface interactions. As a model for better understanding such control of crystal morphology, an α-helical peptide (CBP1) was synthesized having an array of aspartyl residues designed to bind to the {$\bar{1}$10} prism faces of calcite. When added to a saturated solution of calcium bicarbonate containing rhombohedral calcite seed crystals, CBP1 had a remarkable effect on subsequent calcite growth, depending on growth conditions. At 3 °C, where CBP1 is 89% helical, the crystals assumed a prismatic habit, with growth continuing along the *c*-axis, but inhibited parallel to the *c*-axis and prism faces; at 25 °C, where CBP1 is largely unstructured, studded crystals formed, resulting from epitaxial growth off each of the six rhombohedral surfaces. Other acidic peptides also caused similar epitaxial growth. These results suggest that the helical form of the peptide recognizes specific crystal surface characteristics, whereas the unfolded form acts nonspecifically as a polyanion. When the peptide was removed from the growth medium containing either type of crystal, regrowth of {104} rhombohedral surfaces ensued at the expense of the nonrhombohedral surfaces. These results represent the first example of conformation-dependent control of calcite crystal growth by a peptide of defined secondary structure.

Introduction

Biological composites such as bone, teeth, and shells consist of a crystalline inorganic phase within a polymeric organic matrix. The organisms that produce these materials exert an exquisite control over the minerals they deposit, creating materials of myriad shapes and sizes and often high strength. Mineralized tissues are often found to contain polymorphs and individual minerals whose crystal morphology, size, and orientation are determined by local conditions and, in particular, the presence of "matrix" proteins or other macromolecules.[1] The processes and materials that control such crystal growth are of great interest to materials scientists who seek to make composite materials and crystalline forms analogous to those produced by Nature.[2]

Although some 60 minerals of biological origin are known, calcite and aragonite, two polymorphs of $CaCO_3$, are by far the most common.[2] Because most biominerals contain acidic matrix proteins or glycoproteins that influence crystal growth,[1] many efforts to mimic the action of matrix proteins have focused on acidic polypeptides such as polyaspartic acid[3] or other polyanions.[4,5] Work by Mann *et al.* has shown that the shape of calcite crystals can be modified by the addition of simple metal cations[6,7] and small α,ω-dicarboxylic acids,[4] but to date no larger molecules have been described that modify crystal morphology *and* have well-defined secondary structure. There exists, however, a well-studied class of polypeptides, namely, the antifreeze polypeptides (AFPs) from cold water fish and other organisms, which alter the shape of ice crystals in addition to lowering the freezing point of water.[8] Of these, the α-helical type I AFP from winter flounder is the most thoroughly studied. The winter flounder AFP is a rigid, 37-residue α-helix with polar side chains on one side of the helix that bind, with a specific orientation, to the {20$\bar{2}$1} hexagonal bipyramidal surfaces of ice and cause ice crystals to grow as hexagonal bipyramids rather than hexagonal plates.[9] Detailed mechanisms for this binding have been proposed.[10,11] The operative principle for freezing point lowering by an AFP is that binding to the {20$\bar{2}$1} (or other) surface inhibits addition of water molecules to this surface; further growth occurs only by addition to the basal and prism surfaces of the hexagonal plate, which become progressively smaller until only {20$\bar{2}$1} surfaces remain. At this point, crystal growth ceases, and the entire crystal surface is comprised of {20$\bar{2}$1} faces.

From insights gained in the study of AFPs,[10,12] we reasoned that it should be possible to construct a polypeptide that could bind to a specific surface of a growing mineral crystal and alter its shape such that the newly expressed surface is that to which the polypeptide is binding. In this report we describe such a peptide and demonstrate that it can indeed alter calcite crystal

* Author to whom correspondence should be addressed.

⊗ Abstract published in *Advance ACS Abstracts,* October 15, 1997.

(1) (a) Simkiss, K.; Wilbur, K. M. *Biomineralization: Cell Biology and Mineral Deposition*; Academic Press Inc.: San Diego, 1989. (b) Lowenstam, H. A.; Weiner, S. *On Biomineralization*, Oxford University Press: New York, Oxford, 1989.

(2) (a) Berman, A.; Hanson, J.; Leiserowitz, L.; Koetzle, T. F.; Weiner, S.; Addadi, L. *Science* **1993,** *259*, 776−779. (b) Mann, S.; Archibald, D. D.; Didymus, J. M.; Douglas, T.; Heywood, B. R.; Meldrum, F. C.; Reeves, N. J. *Science* **1993,** *261*, 1286−1292. (c) Weiner S.; Traub, W. *Philos. Trans. R. Soc. London Ser. B* **1994,** *304*, 425−434. (d) Falini, G.; Albeck, S.; Weiner, S.; Addadi, L. *Science* **1996,** *271*, 67−69. (e) Berman, A.; Ahn, D. J.; Lio, A.; Salmeron, M.; Reichert, A.; Charych, D. *Science* **1995**, *269*, 515−518.

(3) Wierzbicki, A.; Sikes, C. S.; Madura, J. D.; Drake, B. *Calcif. Tissue Int.* **1994,** *54*, 133−141.

(4) Mann, S.; Didymus, J. M.; Sanderson, N. P.; Heywood, B. R.; Samper, E. J.A. *J. Chem. Soc., Faraday Trans.* **1990,** *86*, 1873−1880.

(5) Albeck, S.; Aizenberg, J.; Addadi, L.; Weiner, S. *J. Am. Chem. Soc.* **1993**, *115*, 11691−11697.

(6) Titiloye, J. O.; Parker, S. C.; Osguthorpe, D. J.; Mann, S. *J. Chem. Soc., Chem. Commun.* **1991,** 1494−1496.

(7) Rajam S.; Mann, S. *J. Chem. Soc., Chem. Commun.* **1990,** 1789−1791.

(8) (a) Davies, P. L.; Hew, C. L. *FASEB J.* **1990,** *4*, 2460−2498. (b) Ananthanarayanan, V. S. *Life Sci. Rep.* **1989,** *7*, 1−32. (c) Hew, C. L.; Yang, D. S. C. *Eur. J. Biochem.* **1992,** *203*, 33−42.

(9) Knight, C. A.; Cheng, C. C.; DeVries, A. L. *Biophys. J.* **1991,** *59*, 409−418.

(10) Wen, D.; Laursen, R. A. *Biophys. J.* **1992,** *63*, 1659−1662.

(11) Sicheri, F.; Yang, D. S. C. *Nature* **1995,** *375*, 427−431.

(12) (a) Wen, D.; Laursen, R. A. *J. Biol. Chem.* **1992,** *267*, 14102−14108. (b) Chakrabartty, A.; Ananthanarayanan, V. S.; Hew, C. L. *J. Biol. Chem.* **1989,** *264*, 11307−11312.

S0002-7863(97)02270-1 CCC: $14.00

morphology. The mineral chosen for this study was calcite, the most common biomineral,[13] and one which can be grown easily (as rhombohedra) in the laboratory. We chose the α-helix as the scaffold for the calcite binding peptide (CBP) based on our experience with helical type I AFP analogs[10,12a] and because the α-helix is the easiest of the common secondary structure motifs to construct and characterize.

Experimental Section

Peptide Synthesis. CBP1 and other peptides were synthesized using Fmoc (9-fluorenylmethoxycarbonyl) chemistry on a MilliGen 9050 solid-phase peptide synthesizer.[14] The solid support used was Tentagel S AM resin from Advanced Chemtech (substitution = 0.27 mmol/g). Fluorescent peptides were obtained by coupling Fmoc β-alanine to the N-terminal residue of the completed peptidyl-resin, followed by removal of the Fmoc group and addition of fluorescein isothiocyanate. Before synthesis, a 1-mm × 1-mm piece of peptide synthesis membrane (polypropylene to which is bonded poly(aminoethylmethacrylamide); 022-μm pore size, 300−400 mmol/cm^2)[15] was added to each reaction column to permit simultaneous peptide synthesis on the membrane; the peptidyl membrane was used to confirm the integrity of synthesis by solid-phase sequencing. Following assembly of the peptide chain, peptides were deprotected and cleaved from the resin support by treatment for 4 h with trifluoroacetic acid/triethylsilane (95:5). The reaction mixture was filtered through fine glass wool in a glass pipet and filtrate collected. Trifluoroacetic acid was concentrated at 30 °C under a gentle stream of N_2 gas. Peptides were precipitated by addition of cold anhydrous ethyl ether and collected by centrifugation. After being washed with fresh ether, the peptide precipitates were dried under vacuum and dissolved in water or 0.1 M ammonium bicarbonate buffer; the solution was then frozen and lyophilized. Stock solutions of peptides for crystal modification studies were made by dissolving the lyophilized ammonium salts in water.

Peptide Purification. Analysis and purification of peptides were performed by reversed phase HPLC on Vydac C18 columns (300 Å pore size, 5-μm particle size; 4.6-, 10-, and 22-mm diameter × 250-mm length) with use of a Waters 600E pump and a Waters 486 tunable wavelength detector (for monitoring at 214−237 nm, depending on sample and column size). Peptides were eluted by using a linear gradient of 2−60% B into A over 60 min (A = 0.05% trifluoroacetic acid in water; B = 0.05% trifluoroacetic acid in acetonitrile) at flow rates of 0.9 (4.6-mm column), 1.7−2.5 (10-mm column), and 6−8 mL/min (22-mm column). The desired peaks were collected with a Gilson FC 80 Microfractionator.

Peptide Characterization. A. Mass Spectrometry. Peptide masses were confirmed by MALDI-TOF mass spectrometry on either a Finnigan Lasermat or a PerSeptive Biosystems Voyager DE biospectrometry workstation.

B. Sequence Analysis. Peptide sequences were confirmed via Edman degradation on a MilliGen 6600 ProSequencer. Peptides covalently attached to synthesis membrane were placed in the sequencer after deprotection with trifluoroacetic acid/triethylsilane without further treatment.

C. Amino Acid Analyses. Amino acid compositions and the concentration of stock peptide solutions used for circular dichroism studies and calcite modification experiments were determined by using the Waters Pico-Tag method; 2-aminoadipic acid was used as the internal standard.

D. Circular Dichroism Spectrometry. Circular dichroism spectra were run to determine the α-helical content of peptides. Measurements were made on an Aviv model 62 DS circular dichroism spectrometer equipped with a computer-controlled HAAKE model F3-CH thermostated bath. Spectra were taken routinely at peptide concentrations of about 0.5 mg/mL (0.15 mM) in 0.1 M ammonium bicarbonate buffer (pH ∼7.8) in 0.1- and 1.0-mm path length cells. Run parameters were as follows: resolution = 0.3 nm; bandwidth = 1.0 nm; average scan time = 1.5 s. The helix content was calculated by using the formula of Greenfield and Fasman,[16] except that measurements were made at 222 nm rather than 208 nm;[12] calculation of the molar ellipticity for a theoretical 31-residue, 100% helical peptide was made by using the method of Chen *et al.*[17]

Crystal Growth Experiments. Calcite crystals were grown in hanging drops of saturated $Ca(HCO_3)_2$ solution, prepared essentially according to Mann *et al.*,[4] using Crystal Plate protein crystallization chambers (ICN Pharmaceuticals, Inc.). Glass cover slips were siliconized by using hexamethyldisilazane or Prosil 28 (PCR, Inc.), and 7 to 10 μL of the saturated $Ca(HCO_3)_2$ solution (ca. 6.7 mM, pH ∼6.2) was placed on a cover slip, which was then inverted over a Crystal Plate well containing 10 μL of water and was sealed with silicone grease. This setup allows each individual drop to be sealed in a separate chamber with its own microenvironment; the water traps CO_2 which diffuses out of the bicarbonate solution. After 15 min, the drops were inspected under an optical microscope for seed crystal formation on the glass surface. When rhombohedral seeds became barely visible, the seal to the chamber was broken, 0.5−3 μL of peptide (ammonium salt) solution was added, and the chamber was quickly resealed. The final peptide concentration was generally 0.2−0.35 mM. Crystal growth studies were carried out at 3 °C (in a cold room) and at 25 °C in replicate, using control peptides and various peptide concentrations. Each Crystal Plate allows up to 15 experiments to be carried out simultaneously. After about 24 h (36−48 h at 3 °C), crystals of 10 to 40 μm were obtained. Crystals forming at the air/water interface were not used, because they tended to clump together, resulting in intergrown, irregular shapes. Crystals forming at the glass/water interface tended to be single and well-spaced, and were more easily analyzed. When the crystals were sufficiently large, the seal was broken and the mother liquors and non-adhering crystals were removed by touching the drop to the corner of a wipette. The glass cover slips were then inverted and crystals were washed several times with Milli-Q purified water.

Scanning Electron Microscopy. Crystals were air dried, sputter-coated with gold, and analyzed with a JEOL 6100 scanning electron microscope, operating at 10 kV and equipped with a Kevex energy dispersive X-ray spectrometer for elemental analysis of crystals.

Fluorescence Microscopy. Images of crystals grown in the presence of fluorescein-labeled peptides were obtained without further manipulation by using a Zeiss Axioplan fluorescence microscope, equipped with a photographing station. Imaging was performed by using a fluorescein filter (excitation 450−490 nm; emission 515−565 nm) or a UV filter (365−420 nm).

X-ray Diffractometry. X-ray powder diffraction studies were performed on a Scintag XDS 2000 instrument equipped with a liquid N_2 cooled, high purity germanium low energy photon spectrometer (EG & G Inc.); operating bias of 1500 V (Cu $K\alpha_1$ line; λ = 1.54 Å).

Results

For initial studies we elected to synthesize a peptide designed to bind to the $\{1\bar{1}0\}$ prism faces of calcite, which in principle should produce hexagonal prisms with {104} rhombohedral caps, similar to those reported for calcite crystals grown in the presence of α,ω-dicarboxylic acids,[4] EDTA,[5] and Mg^{2+} ions.[6] The CBP scaffold is basically a polyalanine rod with a C-terminal amide and Asp and Lys residues at the N- and C-termini, respectively, for helix dipole stabilization, as well as a Pro at position 3 to initiate helix formation.[18] The design of a potential calcite binding peptide (CBP1) was based roughly on the structure of the grubby sculpin AFP (GS-5), which is somewhat smaller than the winter flounder AFP. The main difference is that the two putative ice binding motifs (Lys-Thr-Asp) in GS-5 are replaced by two pairs of Asp residues in the

(13) Reeder, R. J. *Carbonates: Mineralogy and Chemistry. Reviews in Mineralogy*, Mineralogical Society of America: Washington, DC, 1983; Vol 11, pp 1−21.

(14) Atherton, E.; Sheppard, R. C. *Solid-Phase Peptide Synthesis: A Practical Approach;* IRL Press: Oxford, New York, 1989.

(15) Wang, Z.; Laursen, R. A. *Peptide Res.* **1992,** *5*, 275−280.

(16) Greenfield, N.; Fasman, G. D. *Biochemistry* **1969,** *8*, 4108−4116.

(17) Chen, Y. H.; Yang, J. T.; Chau, K. H. *Biochemistry* **1974,** *13*, 3350−3359.

(18) (a) Fairman, R.; Shoemaker, K. R.; Stewart J. M.; Baldwin, R. L. *Proteins: Struct. Fun. Genet.* **1989,** *5*, 1−7. (b) Hol, W. G. J. *Prog. Biophys. Mol. Biol.* **1985**, *45*, 149−195.

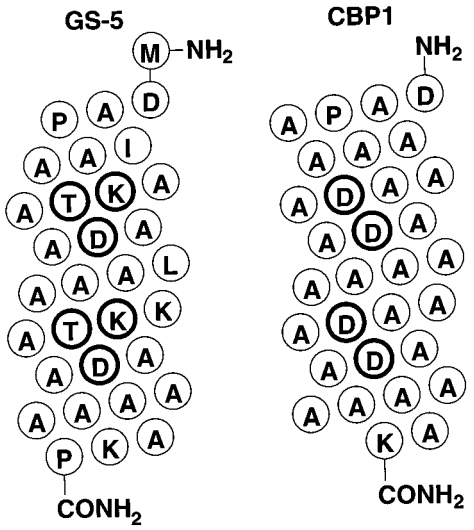

Figure 1. Helix net diagrams of the antifreeze polypeptide GS-5 and of the derived calcite binding peptide, CBP1, showing respectively the putative ice-binding (KTD) and calcite-binding (DD) motifs on one side of each helix.

i and *i* + 3 positions at residues 10 and 13 and 21 and 24 in CBP1 (Figure 1), oriented along one side of the helix so as to occupy carbonate sites on the crystal surface, assuming some mobility of the β-carboxyl groups. In the idealized helix, the distance between the pairs (β-carbons) is 16.5 Å, which approximates a distance between three carbonate layers in calcite of 17.2 Å (Figure 2).

CBP1 and other peptides were synthesized and purified following standard methods.[14] The helix content of CBP1 was determined by circular dichroism spectrometry,[12] which showed 89% helix at 3 °C and 42% at 25 °C. A similar dependence of helicity on temperature has been noted for AFP analogs.[12a] Although circular dichroism measurements were made in ammonium bicarbonate at pH 7.8, we have assumed that the helix content is similar in the $Ca(HCO_3)_2$ crystallization solutions (pH ~6.2), since studies with antifreeze peptides of similar structure show constant helix content over the pH 5−9 range.[12b] These measurements cannot be made on the crystallization solutions directly, because of outgassing of carbon dioxide and crystallization of calcite. It appears that placing Asp carboxylates adjacent to one another in the *i* and *i* + 3 positions does not have a large detrimental effect (i.e., due to repulsion of the carboxylate groups) on helicity.

The effect of CBP1 and other peptides on calcite crystal growth was assessed by adding the peptide to rhombohedral seed crystals growing from a saturated $Ca(HCO_3)_2$ solution at Ca^{2+}/peptide ratios of about 20−30/1. Peptide added directly to $Ca(HCO_3)_2$ solution in the absence of seed crystals generally inhibited crystal growth. Figure 3A shows typical rhombohedral crystals of calcite grown in the absence of peptides; smaller crystals of this type were used as seeds for studies with peptides. When CBP1 was added to seed crystals at 3 °C, and growth was allowed to continue, a marked change in morphology was observed, namely to crystals elongated along the [001] direction (*c*-axis) with rhombohedral {104} caps (Figure 3B). This is the shape that would be expected if growth occurs on the {104} surfaces and is inhibited by binding of the peptide to the prism faces (Figure 4), except that here well-defined prism faces are not seen. When the mother liquor surrounding these "prismatic" crystals was removed and replaced with fresh saturated $Ca(HCO_3)_2$ solution, after washing the crystals with water, the inhibitory effect of CBP1 was lost and a sort of repair process ensued, with subsequent growth occurring on the putative prism

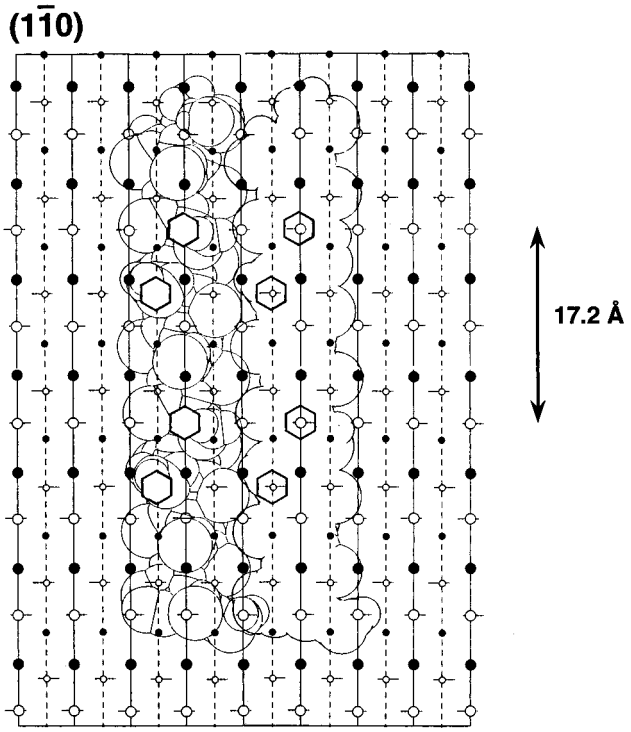

Figure 2. Footprint of two CBP1 molecules binding to the {1$\bar{1}$0} prism faces of calcite. In the left-hand representation the peptide is transparent, with the calcite surface and the the underside of the peptide bearing the calcite-binding Asp side chains visible beneath. Filled circles are Ca^{2+} ions, and open circles are CO_3^{2-} ions. Large circles are ions in the plane of the surface and small circles are 1.28 Å behind this plane. It is proposed that peptide carboxylate ions occupy CO_3^{2-} sites (indicated by hexagons) on this essentially corrugated surface. Note that adjacent peptides can make good van der Waals contact in this arrangement, which may contribute to enhanced binding through cooperative interactions between molecules.

surfaces leading toward a regular rhombohedron (Figure 3C). A very different result obtained when the same series of experiments was carried out at 25 °C, at which temperature CBP1 is only about 40% helical. Under these conditions, epitaxial growth perpendicular to each of the six rhomobhedral surfaces occurred, resulting in studded crystals (Figure 3, parts D and E). When these crystals were washed and allowed to regrow in fresh $Ca(HCO_3)_2$ solution, repair of the non-rhombohedral surfaces was again seen, except that in this case each stud formed a new rhombohedron, resulting in an assembly of six regular rhombohedra overgrowing the original seed (Figure 3F).

Discussion

Alteration of Calcite Crystal Morphology by CBP1. These experiments demonstrate that a polypeptide can have a dramatic effect on calcite crystal morphology and that the effect is conformation dependent. Crystals similar to the prismatic crystals in Figure 3B have been reported for calcite grown in the presence of malonate[4] and EDTA.[5] The latter, like those in Figure 3B, are elongated along the *c*-axis and have rhombohedral caps. But because they do not have well-defined prism faces, it is impossible to conclude whether the additive is binding to the primary {1$\bar{1}$0} or secondary {110} prism faces, although it has been argued,[4] based on model studies, that the dicarboxylates make a better fit to the {1$\bar{1}$0} surfaces than to {110}. Similarly, because of the rounded, irregular shape of the central portion of the crystal shown in Figure 3B, we cannot state at this point whether the newly expressed faces are {1$\bar{1}$0} or {110}

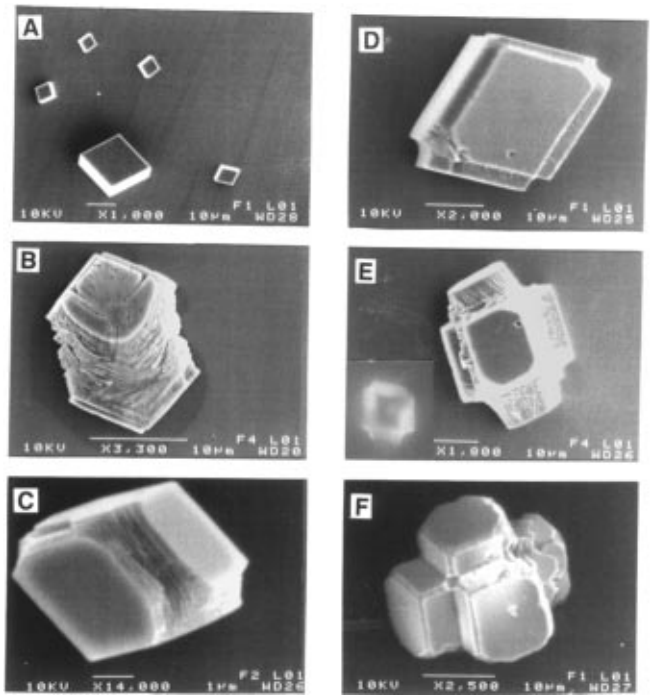

Figure 3. SEM micrographs showing the effect of CBP1 on the growth of calcite crystals. (A) Calcite seed crystals showing typical rhombohedral morphology. (B) Elongated calcite crystals formed from seed crystals at 3 °C in saturated $Ca(HCO_3)_2$ containing ca. 0.2 mM CBP1, showing expression of new surfaces corresponding to the prism faces and rhombohedral {104} caps; growth is along the *c*-axis, which extends through the vertices of the end caps. (C) "Repair" and re-expression of rhombohedral surfaces when crystals from (B) are allowed to grow in saturated $Ca(HCO_3)_2$ after removal of CBP1 solution. (D and E) Respective earlier and later stages of growth of calcite crystals from rhombohedral seed crystals at 25 °C in saturated $Ca(HCO_3)_2$ containing ca. 0.2 mM CBP1, showing epitaxial growth from the rhombohedral surfaces. (E inset) Fluorescence micrograph of epitaxial studded calcite crystals grown under similar conditions in the presence of fluorescein-labeled CBP1; the dark spot in the center corresponds to a (104) face, indicating that the peptide is binding to the newly expressed surfaces and not {104}. Control experiments, in which rhombohedral seed crystals were placed in an exhausted $Ca(HCO_3)_2$ solution containing fluorescein-labeled CBP1 showed no binding to {104} surfaces, although some binding was seen at the crystal edges, which, because of "rounding", presumably expose other surfaces. (F) "Repair" and re-expression of rhombohedral surfaces when crystals from (E) are allowed to grow in saturated $Ca(HCO_3)_2$ after removal of CBP1. All crystal types were confirmed as being calcite by X-ray powder diffraction analysis.

(cf. Figure 4). It is even less clear which surface(s) is being inhibited in the case of the epitaxial, studded crystals (Figure 3E). Growth appears to be in a direction perpendicular to the {104} surfaces to give protrusions that taper toward the ends. Another feature of this growth (cf. Figure 3D) is that that the acute corners of the rhomboid surfaces become truncated, resulting in a hexagonal shape, as if growth is occurring along an axis with hexagonal symmetry. The idea that binding is occurring on the non-rhombohedral surfaces is reinforced by an experiment in which crystals were grown in the presence of CBP1 labeled at the N-terminus with fluorescein. In this case, the same studded crystals were obtained, but fluorescence was seen only on the newly formed non-rhombohedral surfaces (Figure 3E inset). The fact that these crystals fluoresce even after extensive washing indicates that either binding of the peptide is fairly strong or there is overgrowth of the peptide by $CaCO_3$. There is evidence that the latter can occur, because when fluorescent crystals are allowed to regrow in fresh Ca-

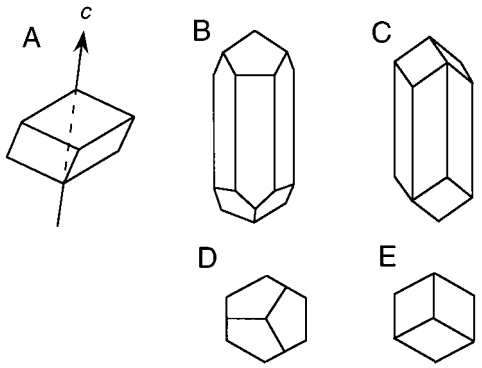

Figure 4. Schematic representation of theoretical calcite morphologies. (A) Typical calcite habit showing the {104} rhombohedral faces. (B) Elongated crystals expressing the {110} primary prism faces. (C) Elongated crystals expressing the {110} secondary prism faces. Note that both elongated forms have {104} rhombohedral end caps. (D and E) Top views, looking down the *c*-axis, of the crystals represented in parts B and C, showing respectively pentagonal and rhomboid {104} faces.

$(HCO_3)_2$ solution, the resulting repaired crystals (not shown, but similar to those in Figure 4F) are also fluorescent. Overgrowth of the peptide is also consistent with earlier observations of the unusual ability of calcite to incorporate polymers such as silica gel[19] and proteins[20] into its crystal lattice. Unfortunately, the same experiment could not be done to generate fluorescent "prismatic" crystals, because the fluoresceinyl group disrupted the helicity of the peptide even at 3 °C, and only epitaxial growth was seen.

The reformation of rhombohedral surfaces after removal of CBP1 can be understood in terms of calcite crystal surface energies. The most common form of calcite is the rhombohedon, because its {104} surfaces are of lowest energy, combining close packing and equal numbers of positively and negatively charged ions on each surface. Under ordinary conditions, other surfaces, such as the $\{1\bar{1}0\}$ prism surfaces or the unidentified surfaces seen in the epitaxial, studded crystals (Figure 3E), would be of higher energy. After removal of the inhibiting peptide, ions will add to the highest energy surface (e.g., $\{1\bar{1}0\}$), filling in the gaps, resulting in re-expression of the lower energy {104} surfaces seen in Figure 3, parts C and F.

At 25 °C, CBP1 is only about 40% helical, suggesting that CBP1 may be binding to calcite simply as a polyanion, rather than as a peptide with definite structure. In fact, we found a number of other anionic peptides that cause epitaxial, studded growth, rather than "prismatic", including Ac-EPAAAAAE-ADAKDAAAAAAADEADAKAAK, an unsuccessful CBP candidate with low helicity, and the nonhelical peptide SYD-PYASLEDPDSEQSK (unpublished observations). When the Asp and Glu groups of the latter were substituted with Asn and Gln, respectively, the resulting neutral peptide had no effect at all on calcite morphology: only rhombohedra like those in Figure 3A were observed. Several other anionic peptides, and even polymethylmethacrylate, were found to cause epitaxial growth, whereas neutral and basic peptides did not (unpublished observations).

Matrix Proteins and Calcite Morphology. The matrix proteins of mollusc shells and the exoskeletons of other marine organisms are typically polyanionic, having a high content of aspartic and glutamic acid and phosphoserine residues,[5,21] as might be expected for calcium binding proteins. The matrix proteins and the cells that produce them have a profound

(19) Henisch, H. K. *Crystal Growth in Gels*; Pennsylvania State University Press: University Park, PA, 1970; pp 63−71.
(20) Berman, A.; Addadi, L.; Weiner, S. *Nature* **1988,** *331,* 546−548.

influence on the shape and properties of calcite crystals formed in their presence.[2a] For example, sea urchin spicules are single crystals of calcite, yet their shape is not rhombohedral, but rather has a complex "cactus-like" appearance. Furthermore, these crystals do not cleave along the {104} rhombohedral cleavage planes, but break with a conchoidal (glassy) fracture typical of an amorphous material. This appears to be due to the unusual property of calcite of being able to incorporate the matrix protein into its crystal lattice, giving it added strength.[20]

The results of studies with matrix proteins isolated from marine organisms are sometimes difficult to interpret at the molecular level, because neither the matrix proteins themselves nor the new calcite surfaces formed in their presence are easy to characterize. Nevertheless, it is clear that matrix proteins influence calcite crystal morphology. For example, Albeck *et al.*[5] have reported that calcite crystals grown in the presence of sea urchin matrix protein bind to calcite faces (presumably prism) lying parallel to the *c*-axis, as we report here (Figure 3B); on the other hand, they found that different matrix protein fractions from a mollusk bound either the (001) basal faces or surfaces parallel to the *c*-axis. Wierzbicki *et al.*[3] have concluded that oyster shell matrix protein binds to the $\{1\bar{1}0\}$ surface, based on atomic force microscopy and computational analysis. Nucleation off the (001) basal face is thought to be a common occurrence in biomineralization, and it has been suggested that acidic nucleating proteins may adopt a β-sheet structure, with the anionic groups on the nucleating face of the sheet and hydrophobic groups, bound to an underlying substrate, on the other.[21a] Although Weiner and Traub[22] have reported that certain mollusc shell matrix proteins have β-sheet content, based on X-ray fiber diffraction methods, no detailed matrix protein structure (e.g., X-ray crystal structure) has yet been determined.

Other Biomineralization Model Systems. There have been numerous approaches to devising biomineralization models. Addadi *et al.*[23] reported that polyaspartic acid adsorbed on sulfonated polystyrene surfaces assumes a β-sheet conformation and nucleates calcite growth by binding to the (001) surface. On the other hand, Wierzbicki *et al.*[3] argue for binding of $(Asp)_{15}$ to $\{1\bar{1}0\}$ in crystals grown in solutions containg $(Asp)_{15}$. Wheeler and Sikes[21b] have shown that synthetic peptides containing $(Asp)_n$ can inhibit calcite growth and nucleation, but in this case no information relating secondary structure to function was reported. Perhaps the best characterized nucleating surface is that provided by oriented films of polymeric pentacosadiynoic acid, which cause calcite to nucleate off a (012) second-order rhombohedral face.[2e]

Mann and co-workers have examined the effect of small molecule models on calcite crystal growth. In a study of dicarboxylic acids, they found that calcite crystals grown in the presence of malonic, aspartic, and γ-carboxyglutamic acid all displayed prismatic faces, indicating binding to the $\{1\bar{1}0\}$ surfaces, and they proposed specific sites on the $\{1\bar{1}0\}$ faces where the carboxylates could bind to calcium atoms.[4] Crystallization of $CaCO_3$ under compressed monolayers of negatively charged stearic acid gave both calcite and the relatively unstable vaterite, depending on calcium concentration.[24] At the highest concentrations of $[Ca^{2+}]$, oriented nucleation was induced primarily on the $\{1\bar{1}0\}$ faces of calcite, along the *c*-axis and parallel to the monolayer/solution interface. This result was interpreted in terms of a close match between calcium atoms on the $\{1\bar{1}0\}$ surface and stearate head groups arranged in a hexagonal closest packing array.[24] The same investigators have shown that Mg^{2+} and Li^+ stabilize the $\{1\bar{1}0\}$ and (001) surfaces, respectively.[6,7]

Until now, there have been no published reports describing the alteration of calcite crystal morphology by natural or synthetic polypeptides having *well-defined* secondary or tertiary structures. The best evidence suggests that at least some natural matrix proteins may contain β-sheet structure, but peptide models with discrete β-sheet structures (as opposed to polyamino acids or peptide aggregates with bulk β-structure) are notoriously difficult to construct. On the other hand, the α-helix is one of the easiest secondary structure elements to synthesize and characterize. For this reason, and because of the analogy with antifreeze proteins, we chose the α-helix as the basis for synthesis of a calcite binding peptide, even though there is no evidence that natural matrix proteins are helical.

Conclusions. We have shown here that a single peptide can have a remarkable effect on calcite morphology, with at least three different shapes being produced depending on peptide conformation and other conditions. These observations should help in understanding how an organism can control crystal morphology using specific matrix molecules and environmental conditions (pH, concentration, etc.), or a sequence of changes, leading to the varied and intricate shapes seen in Nature.[2ab] Work is currently underway to characterize the new crystal surfaces being expressed, as well as the nature of their interaction with CBP1, and to synthesize peptides that may cause expression of other surfaces. CBP1 also represents a rare example of a peptide structure designed *de novo* to carry out a function in a manner that has no natural counterpart, since no α-helical peptide or protein has so far been implicated in the process of biomineralization. The chemical re-engineering of a peptide that modifies ice morphology to one that alters the shape of a mineral is analogous to natural evolutionary processes, whereby numerous proteins, through mutation, have acquired new functions.

Acknowledgment. This work was supported by a grant (DAAH04-94-G-0308) from the Army Research Office. We wish to thank Dr. William Croft of the Harvard University Mineralogical Museum for providing X-ray diffraction facilities and other advice on crystal characterization.

JA972270W

(21) (a) Addai, L.; Weiner, S. *Angew. Chem., Int. Ed. Engl.* **1992,** *131,* 153−169. (b) Wheeler, A. P.; Sikes, C. S. In *Materials Synthesis Utilizing Biological Processes;* Rieke, P. C., Calvert, P. D., Alper, M., Eds.; Materials Research Society: Pittsburgh; pp 45−50.

(22) Weiner, S.; Traub, W. *FEBS Lett.* **1980,** *111,* 311−316.

(23) Addadi, L.; Moradian, J.; Shay, E.; Maroudas, N. G.; Weiner, S. *Proc. Natl. Acad Sci. U.S.A.* **1987**, *84,* 2732−2736.

(24) (a) Rajam, S.; Heywood, B. R.; Walker, J. B. A.; Mann, S.; Davey, R. J.; Birchall, J. D. *J. Chem. Soc., Faraday Trans.* **1991,** *87,* 727−734. (b) Heywood, B. R.; Rajam, S.; Mann, S. *J. Chem. Soc., Faraday Trans.* **1991,** *87,* 735−743.